A standardized and modular power electronics platform for academic research on advanced grid-connected converter control and microgrids

Frank S.R., Schulz D., Stefanski L., Schwendemann R., Hiller M.
Karlsruhe Institute of Technology (KIT), Institute of Electrical Engineering (ETI)
Kaiserstraße 12
Karlsruhe, Germany
Phone: +49 721 608 42465
Email: s.frank@kit.edu
URL: http://www.kit.edu

Acknowledgments

This work was supported by the KIT Future Fields Stage 2 funding program.

Keywords

≪Microgrid≫, ≪Standardization≫, ≪Hardware≫, ≪Grid-forming converters≫, ≪Grid-connected converter≫, ≪Measurements≫, ≪Compensation≫, ≪Harmonic Injection≫, ≪Active damping≫, ≪Smart grids≫, ≪Active Front End≫, ≪LCL≫, ≪Isolated Converter≫

Abstract

This paper introduces a multifunctional converter platform rated at 30 kW. Individual units allow research on advanced grid-connected converter control, while their interconnection enables isolated microgrid investigations. The standardized and modular design allows simple reconfiguration of the system for different setups, for which multiple measurements are presented.

Introduction

As the electrical grid evolves from a system supported by power generation using synchronous generators to rising levels of renewable energy and thus power electronics interfaced power sources, the design, control and coordination of grid-connected power converters are crucial for this ongoing power system evolution.

The microgrid paradigm [1] has established itself as the main approach to operate multiple power converters in a concerted manner. Microgrids consist of multiple converters that allow decentralized grid control, coordination of local energy balance and possible islanding in case of failure of the main grid. Three main aspects are particularly relevant when considering microgrids for research purposes. First, they enable the investigation of a concerted operation of grid-connected converters in a full converter-based microgrid with the above mentioned advantages. Second, an isolated microgrid can be used to emulate arbitrary grid conditions, such as distorted or weak grids, as well as voltage and frequency deviations. Stricter grid connection standards defined for example in [2] and [3] require some degree of grid support in reaction to such deviations, while also specifying necessary Fault-Ride-Through (FRT) capabilities. These can be implemented and examined in the stand-alone microgrid. The isolated microgrid is also beneficial to investigate converters and their controls operating in a grid-forming mode. This includes the necessary synchronization and load sharing between grid-forming units, as well as appropriate short-circuit current limiting. Third, a microgrid provides a testbed for converter-dominated grids facing challenges such as a lack of inertia, overcurrent protection and instability phenomena arising from converter interaction [4].

In literature, several power electronics platforms or testbeds are introduced, developed by various universities and research institutions. In [5], a digital-physical hybrid real-time simulation platform is proposed, [6] presents a platform based on an OPAL-RT simulator and different converters. In [7], [8] and [9] microgrid testbeds are presented to study the interconnected operation of various distributed generators and energy storage. However, most of these platforms utilize commercial power electronics or signal processing subsystems. The disadvantage of this approach is that the system is not cost effective, expensive to maintain or upgrade and modification might not be possible [6]. To avoid these problems and gain full control over the complete system it is therefore expedient to design and construct a platform with self-developed fundamental building blocks.

This paper presents a Standardized Power Electronic Converter Cabinet (SPECC) as building block for a microgrid to take advantage of the aforementioned research benefits. Apart from the microgrid application, the SPECC is intended to offer a platform for general grid-connected converter investigations, including harmonic current mitigation resulting from distorted grid voltages. Due to more restrictive grid codes as well as more demanding size and cost requirements of the converters, LCL line filters are typically employed to reduce current harmonics near the switching frequency. However, possible instabilities due to the filters resonance must be addressed with damping techniques, especially when multiple grid-connected converters with LCL filters are nearby and may affect each other [10].

The developed SPECC-based converter platform provides a testbed for all these investigations under real-world conditions. Its modular design together with the completely self-developed hard- and software enables simple reconfiguration and extension and will be presented in the following section. Thereafter, the standardized measurement acquisition and signal processing system is detailed together with its benefits in the next section. Finally, possible control strategies and associated measurements are shown in the last two sections.

Topology and Hardware Platform

Due to their simple design, low need for semiconductor switches and well-established control, two-level converters are widespread and sufficient for most applications. Therefore, the topology of one SPECC, shown in Fig. 1, is based on standard Two-Level Voltage Source Converters (2L-VSC). It consists of two AC/DC 2L-VSCs at both AC-sides, shown in red. The first DC link (DC1) can be either directly connected to the secondary side (DC2) of a Dual Active Bridge converter (DAB), depicted in blue, or a DC/DC converter, shown in green, can be switched in between. The DC link of the second AC/DC 2L-VSC (DC3) is directly connected to the DABs primary side. The DAB ensures a galvanic isolation between its primary and secondary DC side that allows the realization of galvanically isolated microgrids. The optional DC/DC converter can be used to variably adjust the DABs secondary DC voltage to reach its most efficient operating point or to provide a connection for a DC grid with a specific voltage.

The DAB has been internally developed and used for research before [11], [12]. It consists of two full-bridge units, equipped with Infineon FF23MR12W1M1B11 Silicon Carbide (SiC)-Metal-Oxide Field-Effect Transistor (MOSFET) half-bridge modules, coupled by a Medium Frequency (MF)-transformer. This setup allows a bidirectional power transmission of 30 kW. For the AC/DC 2L-VSC and the DC/DC converter the internally developed 'combi single board converter (combi-EPSR)' introduced in [13] is used. The converter can be either equipped with Cree/Wolfspeed CCS050M12CM SiC-MOSFET or Infineon FS75R12K Silicon (Si)-Insulated-Gate Bipolar Transistor (IGBT) semiconductor modules. In the following, a setup with one SiC-MOSFET combi-EPSR (AC/DC converter 1) switched with $f_{\mathrm{sw,SiC}} = 50\,\mathrm{kHz}$ and one Si-IGBT combi-EPSR (AC/DC converter 2) switched with $f_{\mathrm{sw,IGBT}} = 10\,\mathrm{kHz}$ is used, to evaluate the different behaviour of these technologies in further research. For this reason, two different LCL line filters are used with their parameters given in table I.

For Electromagnetic Compatibility (EMC) reasons two serial connected common mode chokes WE744839010400 with 10.5 mH common mode inductance and 40 A rated current are integrated on both sides between the LCL filters and the combi-EPSRs. Besides the two three-phase AC terminals (AC1 and AC2), the DC terminals of both DAB sides (DC2 and DC3) as well as the output of the

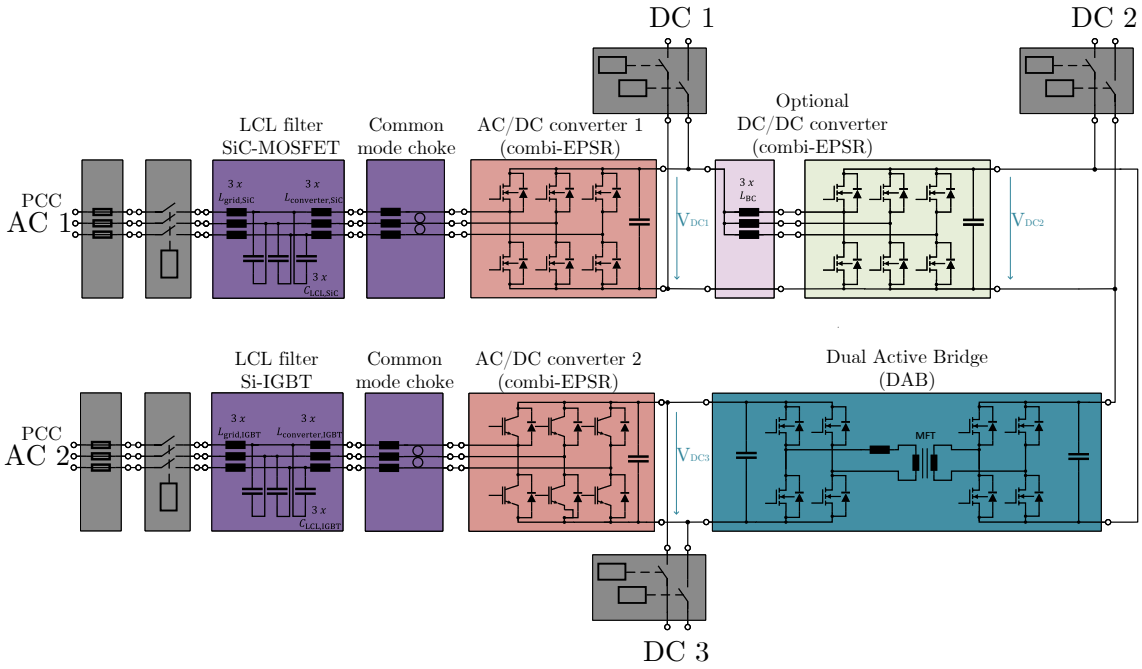

Fig. 1: Topology of one Standardized Power Electronic Converter Cabinet (SPECC)

Table I: Characteristics of the LCL line filters.

LCL filter type	Grid-sided inductance	Converter-sided inductance	Capacitance	Resonance frequency	Current rms	Dimensions	Mass
	L_{grid}	$L_{\text{converter}}$	C_{LCL}	f_{res}	$I_{\text{ph,rms}}$	$l \times w \times h$	
Si-IGBT LCL	$3 \times 150\,\mu$H	3×1 mH	$3 \times 6\,\mu$F (delta)	3.28 kHz	45 A	$260 \times 275 \times 173$ mm	17.5 kg
SiC-MOSFET LCL	$3 \times 50\,\mu$H	$3 \times 100\,\mu$H	$3 \times 4.7\,\mu$F (delta)	7.34 kHz	45 A	$253 \times 196 \times 128$ mm	5.7 kg

DC/DC converter (DC1) are accessible to offer the possibility for DC grid connections. The setup allows DC voltages up to 800 V. First measurements are done without the optional DC/DC converter, resulting in $V_{\text{DC2}} = V_{\text{DC3}}$. The whole setup is pictured in Fig. 2. All power electronics units (DAB and combi-EPSRs) are realized with double-height Eurocard Printed Circuit Boards (PCBs) [14], that are mounted in 19" racks in the lower region of the cabinet. The Central System-on-Chip (SoC)-based signal processing and Control Unit (CCU) and a status panel are placed spatially separated in the upper region. A computer functioning as Human Machine Interface (HMI) and interface to other SPECCs is also placed in this region. It can be operated using a touchscreen or a remote desktop connection. This arrangement ensures the separation of different function units and voltages levels a well as EMC. The mid part of the cabinet offers space for optional project-specific power electronics.

Sensors and Signal Processing

To enable the investigation of advanced control methods for grid-connected converters, each SPECC is equipped with a large number of sensors to measure the voltages and currents of each power electronics unit (DAB and combi-EPSR) as well as the grid currents at the AC terminals i_{grid} and the capacitor voltages v_{c} of the LCL filter.

Since a SPECC employs undamped LCL filters for both the IGBT and SiC AC/DC converter, the possibility of resonances needs to be considered in the controller design. Therefore, additional measurements such as capacitor voltages or capacitor currents are necessary. These measurements can be used to dampen LCL oscillations using appropriate feedback structures. With the measured quantities shown

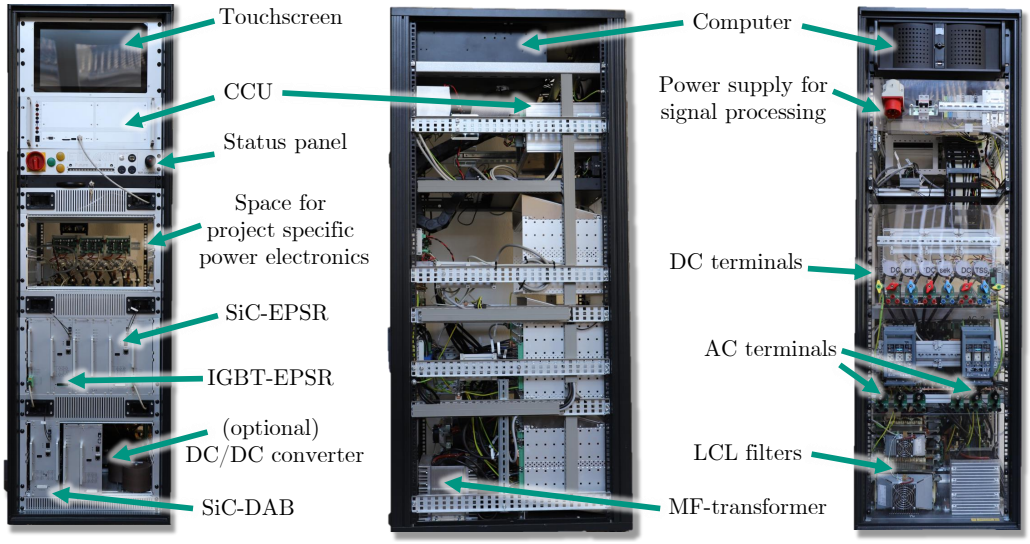

Fig. 2: Hardware setup of the Standardized Power Electronic Converter Cabinet (SPECC)

Table II: Measured Voltages and Currents

Physical quantity	Grid current	Capacitor volt. LCL	AC phase cur. EPSR	DC cur. DAB	AC cur. DAB	Phase volt. EPSR	DC volt. EPSR	DC volt. DAB
	i_{grid}	v_{C}	$i^{\star}_{\text{ph,EPSR}}$	$i^{\star}_{\text{DC,DAB}}$	$i^{\star}_{\text{AC,DAB}}$	$v^{\star}_{\text{ph,EPSR}}$	$v^{\star}_{\text{DC,EPSR}}$	$v^{\star}_{\text{DC,DAB}}$
Measuring range	±102.4 A	±1000 V	±80 A	±160 A	±163.8 A	±600 V	0..1000 V	0..1100 V
Resolution	3.1 $\frac{\text{mA}}{\text{bit}}$ (16 bit)	30.5 $\frac{\text{mV}}{\text{bit}}$ (16 bit)	39 $\frac{\text{mA}}{\text{bit}}$ (12 bit)	78 $\frac{\text{mA}}{\text{bit}}$ (12 bit)	80 $\frac{\text{mA}}{\text{bit}}$ (12 bit)	293 $\frac{\text{mV}}{\text{bit}}$ (12 bit)	488 $\frac{\text{mV}}{\text{bit}}$ (12 bit)	537 $\frac{\text{mV}}{\text{bit}}$ (12 bit)
Sample rate	5 MSPS	5 MSPS	650 kSPS	650 kSPS	1 MSPS	650 kSPS	650 kSPS	650 kSPS

in Tab. II, both the capacitor voltages v_{C} and capacitor currents i_{C} are available. In the current state of development, the capacitor currents are used for the active damping approach, which are calculated using

$$i_{\text{C}} = i_{\text{grid}} - i_{\text{ph,EPSR}}, \tag{1}$$

with the measured grid currents i_{grid} and phase currents $i_{\text{ph,EPSR}}$ of the respective three-phase converter.

The large number of accessible measurements allows the implementation of various control strategies and ensures a save operation of each power electronics unit. Besides, the temperatures of the LCL-filters, MF-transformer and semiconductor modules can be observed, guaranteeing global supervision and safe operation of the whole system.

The signal processing tasks necessary within the SPECC are distributed on multiple layers and processing units, which is shown in Fig. 3. The core of the signal processing architecture is the CCU depicted in Fig. 4, that is based on a *ZYNQ7030* SoC, which consists of two ARM processor cores together with an Field Programmable Gate Array (FPGA). The CCU has eight slots for miscellaneous extension cards, e.g. for fast analogue signal sampling, fiber wire communication and as interface to peripheral components. A detailed description is given in [15]. The FPGA allows a fast reaction to error states, the implementation of low-latency control algorithms and low-level interfacing of the previous mentioned extension cards. The first ARM core is tasked with handling the network communication over TCP/IP. The second ARM core is used to execute control algorithms, to coordinate the overall system using state machines and to perform a safe and controlled system shutdown in case a subsystem reports a fault.

The supervising control and data acquisition tasks are performed by a LabView-based Monitor Control Tool (MCT) on a desktop computer. This computer is located in the same network as the CCU(s), such that both measurement data and control commands can be sent over ethernet connections. Since each SPECC uses the identical signal processing system, the central MCT instance can facilitate communi-

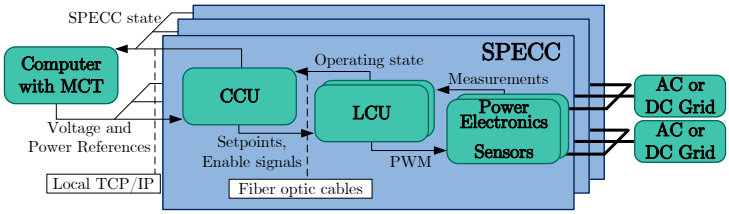

Fig. 3: Hierarchy and interconnections of the signal processing structure

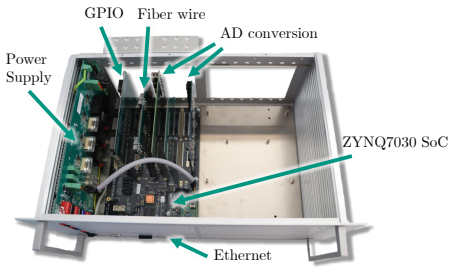

Fig. 4: CCU, based on a *ZYNQ7030* SoC

cation between individual SPECCs. This enables the coordination of multiple SPECCs as required for cooperative operation such as in a microgrid setup.

The lowest layer of the signal processing structure shown in Fig. 3 is formed by Local Control Units (LCU). These are circuit boards equipped with an Artix-7 FPGA that provides signal processing capabilities with minimum signal paths and latency for the associated power electronics. Functionalities implemented on the LCUs include fault detection, for instance overcurrents, overvoltages and overtemperatures as well as high-bandwidth control loops and modulation for the connected semiconductor switches. In a SPECC, both AC/DC converters, the DAB and the optional DC/DC converter each possess a dedicated LCU. The quantities marked with "⋆" in Tab. II are measured, digitized and processed directly on the respective power electronics unit, the other quantities are centrally digitized on the CCU.

Control

A SPECC employs a distributed control architecture that mirrors the signal processing hierarchy presented in Fig. 3. The main design principle for this architecture is the ability of each individual power electronics unit (DAB and combi-EPSR) to control its outputs according to setpoints specified by higher-level control units. For this purpose, the control algorithms can either be executed on the associated LCU or alternatively on the CCU. An overview of several control methods for the operation within the SPECC that are implemented so far is given in Fig. 5.

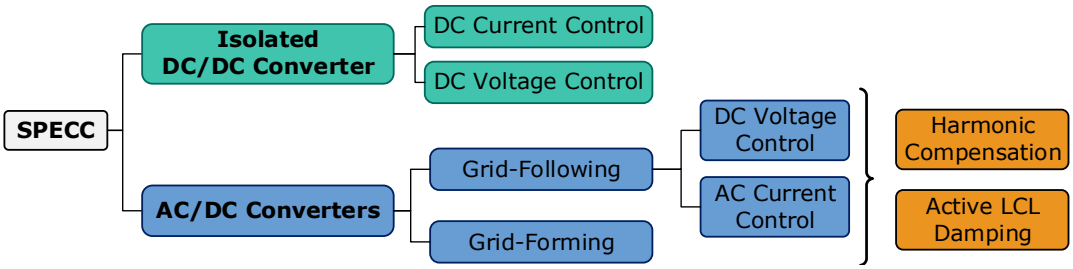

Fig. 5: Overview of control methods used within the SPECC

The interconnection, coordination and interaction of converter systems can be investigated together with the reaction of the converter system to different grid situations. At the same time, the control methods themselves are research subjects. The SPECC provides a platform for the investigation of possible control strategies including resonant controllers, harmonic compensation techniques and active LCL damping approaches.

The control of the single-phase DAB is based on the phase shift φ between the primary-side and secondary-side H-bridge voltage. In [16], the transferred power for single-phase-shift modulation and a MF-transformer with a turns ratio of $n = 1:1$ is derived from the characteristic DAB current and voltage waveforms to

$$P_0 = \frac{{V_S}^2}{\omega L_\sigma} \cdot d \cdot \varphi \cdot \left(1 - \frac{\varphi}{\pi}\right). \tag{2}$$

Ideal semiconductors and an instantaneous current commutation are assumed. For the presented topology with $P_0 = P_{DC}$, $V_S = V_{DC3}$, $d = V_{DC2}/V_{DC3}$ and $\omega = 2\pi \cdot f_{sw}$ follows for both power directions:

$$P_{DC} = \frac{V_{DC2} V_{DC3}}{2\pi f_{sw} L_\sigma} \cdot \varphi \cdot \left(1 - \frac{|\varphi|}{\pi}\right), \tag{3}$$

with the DC voltages on the primary and secondary side V_{DC3} and V_{DC2}, the switching frequency f_{sw} and the leakage inductance L_σ. The specified DC power or current setpoint can be achieved by adjusting the phase shift φ accordingly. Alternatively, the DAB can be operated in a voltage controlled mode. In this case, the phase shift φ is the output variable of a PI controller, which acts on the error between the voltage setpoint and voltage measurement.

The control strategies for the AC/DC converters are mainly distinguished between grid-forming and grid-following operation. First, the control options for the grid-following mode are described. In this case, the three-phase grid currents are the controlled quantities. Additionally, the active current setpoint may be specified by a superimposed control loop that regulates the voltage of the DC link. This control structure is shown in Fig. 6. The current setpoints in the rotating dq-reference frame are transformed into the stationary $\alpha\beta$ frame using the grid angle γ obtained by a Phase-Locked Loop (PLL). The error in the grid currents is then fed into a dampened Proportional-Resonant (PR) controller tuned to the grid frequency of 50 Hz. Additional resonant paths tuned to multiples of the grid frequency can be connected in parallel to the fundamental PR controller as harmonic compensators to attenuate harmonic currents [17]. The resulting controller is described by

$$G_{PR,\,HC}(s) = K_p + \frac{2K_i s}{s^2 + 2\omega_c s + \omega_0} + \sum_{h=7,11,13,17} \frac{2K_{ih}\omega_{ch} s}{s^2 + 2\omega_{ch} s + (h\omega_0)^2}, \tag{4}$$

where K_p is the proportional gain, K_i the resonant gain, ω_0 the grid frequency and ω_c the damping coefficient. Parameters with the additional subscript h denote identical quantities for the aforementioned harmonic compensator terms. The measured grid voltages can be fed forwarded to the controller output. In order to dampen potential oscillations arising from the LCL grid filters, the LCL capacitor currents are also measured and can be utilized for a proportional active damping feedback with a gain of K_{AD}. Both the outer current loop gain K_p and the active damping gain K_{AD} are tuned to ensure stable system poles using root locus analysis [10]. Finally, the calculated output voltage is translated into power electronics switching states by zero sequence Pulse-Width Modulation (PWM).

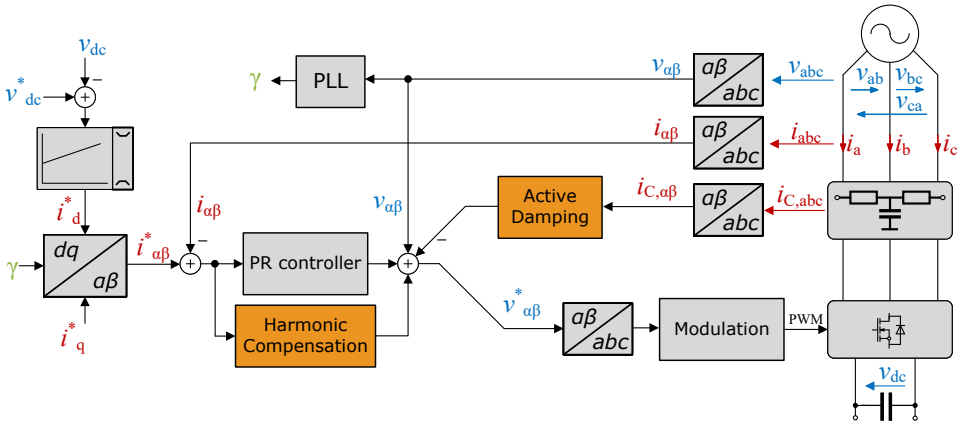

Fig. 6: Control structure for grid-connected AFE with harmonic compensation and active damping

The SPECC is also intended to be used as a research platform for the investigation of grid-forming controls. In this mode, the the three-phase grid voltages at the Point of Common Coupling (PCC) are the control objective. In case the converter system is connected to an existing grid with a voltage system present, the grid-forming control needs to synchronize to the grid angle and adapt its voltage setpoints

using droop controls. Alternatively, in the islanded microgrid case where no other voltage source is connected to the grid, the control needs to be able to regulate the grid voltage on its own. In both cases, either the DC link connectors or the secondary AC connection of the SPECC is used to supply the necessary power for the operation as a grid-forming converter. The overall control setup for the grid-forming operation with a power supply from the laboratory grid is depicted in Fig. 7 with the control objectives shown in black. The same figure shows an alternative application of the SPECC operating as two constant power loads in an existing DC grid.

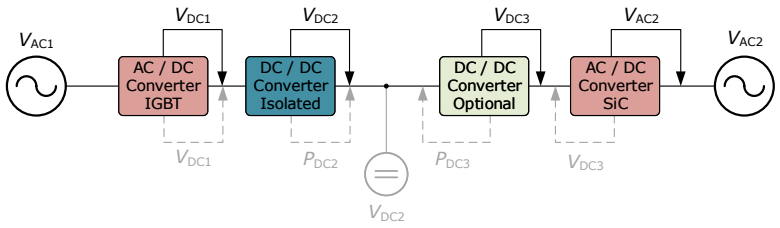

Fig. 7: Control setup within one SPECC. Control objectives shown in black are for grid-forming operation, gray quantitites below are control objectives when operating as constant power load in a DC grid

Measurements

This section will present first measurements taken with the SPECC. First, the application as a platform for the investigation of control methods for grid-connected power converters is demonstrated. Fig. 8 shows the measurements of the AC/DC converter operating as Active Front End (AFE) in a grid-following mode controlling its DC link voltage. Depicted are the phase currents i_a, i_b and i_c, phase voltage v_a, as well as the DC current i_{DC} and DC voltage v_{DC}. In fig. 8(a), the DC voltage setpoint is changed from $v_{DC} = 600\,V$ to $700\,V$ at $t = 16\,ms$. Fig. 8(b) shows multiple load steps. The DC load current as disturbance variable is first reduced to zero at $t = 5\,ms$ and then set to $i_{DC} = 12\,A$ at $t = 10\,ms$. In this application, the SPECC serves to verify the design of both the DC voltage controller and AC current controller, including their optimized controller parameters, real-world performance and controller robustness.

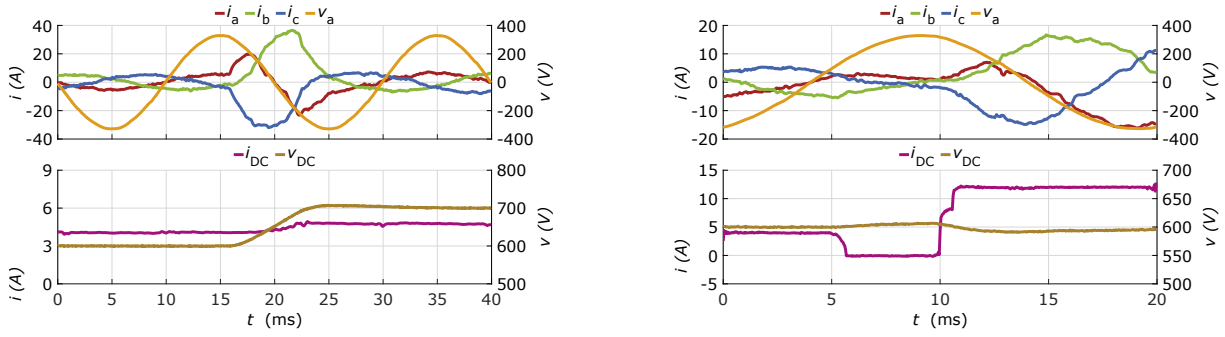

(a) Setpoint step

(b) Load step

Fig. 8: Measurements of AFE DC voltage control with step responses

Apart from the conventional PI and PR controllers under investigation, the SPECC is also able to provide a testbed for more advanced controller structures. One such extension is the addition of harmonic current compensators as described in the control section. The harmonic currents are caused by the harmonic distortions of the grid voltages. This grid may either be the laboratory grid, which already presents distorted grid conditions, or alternatively the isolated microgrid with adjustable voltage distortions. Fig. 9 and 10 show the effect of compensators for the 7th, 11th, 13th and 17th current harmonic, with the grid-side phase currents i_{on} and i_{off} for activated and deactivated harmonic compensation. The Total Harmonic Distortion (THD) is reduced from 0.58 % to 0.15 %.

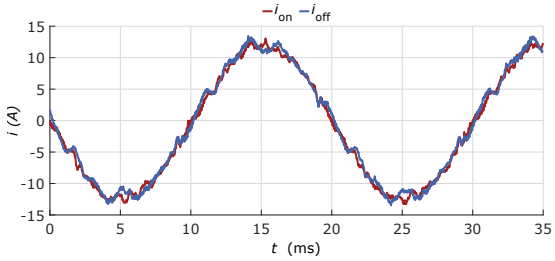

Fig. 9: Measurement of harmonic compensator effect on grid current waveform

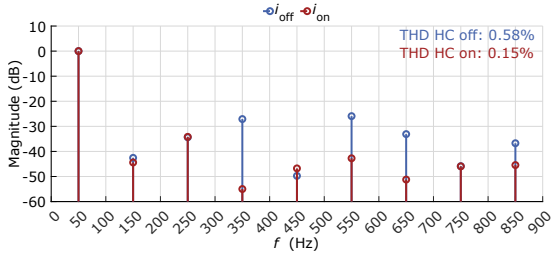

Fig. 10: Measurement of harmonic compensator effect on grid current spectrum

With no passive damping used in the LCL filters on both the SiC and IGBT side, the SPECC allows the examination of active resonance damping approaches described in the previous section. In Fig. 11 the effect of active damping on the capacitor current is illustrated. Depicted are the phase current i_a and line-to-line voltage v_{ab}. At $t = 17\,\text{ms}$ the active damping is disabled. Due to the high bandwidth of the current controller, an oscillation occurs immediately and the system must be switched off.

For the grid-forming operation, first measurements were taken for the most basic case in which only one converter is tasked with regulating the grid voltage, which is depicted in Fig. 12. The grid-forming converter is connected to an ohmic load of $R_{LL} = 146\,\Omega$ and its setpoint increased from $v^*_{LL,1} = 200\,\text{V}$ to $v^*_{LL,2} = 250\,\text{V}$.

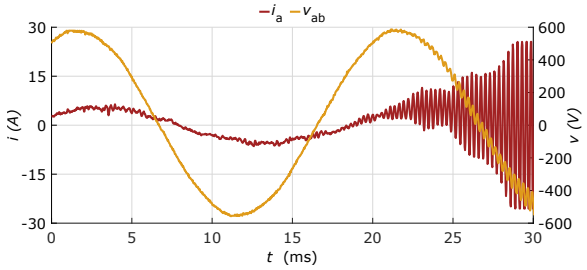

Fig. 11: Measurement of active damping effect

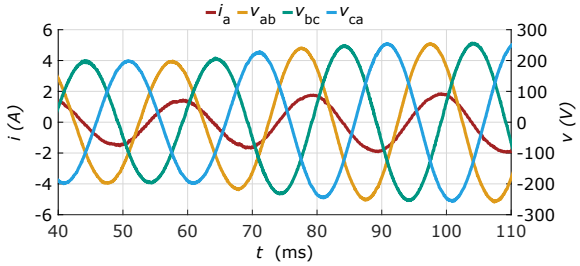

Fig. 12: Measurement of grid forming voltage step

Conclusion and Future Work

This paper introduces a standardized and modular converter platform based on so-called SPECCs. The SPECC, consisting of two AC/DC converters, an isolated DC/DC converter and a standardized signal processing system is well-suited for numerous research applications in the field of grid-connected converter control and microgrids. Measurements demonstrate the function of harmonic compensation and active damping controls. Finally, a basic grid-forming control is also verified with an ohmic load. The shown measurements form the basis for further research on islanded microgrids and the behavior of their converters.

Future work includes studies on the active damping of LCL filters such as capacitor voltage feedback, replacement of capacitor measurements with estimators and state-space control. Apart from harmonic voltage distortions, other typical grid disturbances such as voltage dips, unbalances and changes of grid impedance and their effects on the control stability need to be considered. Furthermore, the coupling of several SPECCs on both the AC and DC side to form AC and DC power electronics based microgrids will be realized. These can then be used to investigate the operation of such isolated microgrids, grid-forming converter controls, converter interactions and possible instabilities in power electronics grids.

References

[1] N. Hatziargyriou, Ed., Microgrid: architectures and control. Chichester, West Sussex, United Kingdom: Wiley, 2013

[2] DIN VDE V 0124-100:2020-06, "Grid integration of generator plants - Low voltage - Test requirements for generator units to be connected to and operated in parallel with low-voltage distribution grids"

[3] VDE-AR-N 4105:2018-11, "Generation Plants on the Low-Voltage Grid - Minimum Technical Requirements for Connection and Parallel Operation of Generation Plants on the Low-Voltage Grid"

[4] Q. Peng, Q. Jiang, Y. Yang, T. Liu, H. Wang, F. Blaabjerg, "On the Stability of Power Electronics-Dominated Systems: Challenges and Potential Solutions", IEEE Trans. on Ind. Applicat. 55, 2019, pp. 7657–7670.

[5] C. Mao et al., "A 400-V/50-kVA Digital–Physical Hybrid Real-Time Simulation Platform for Power Systems," in IEEE Transactions on Industrial Electronics, vol. 65, no. 5, pp. 3666-3676, May 2018

[6] W. Liu, J. -M. Kim, C. Wang, W. -S. Im, L. Liu and H. Xu, "Power Converters Based Advanced Experimental Platform for Integrated Study of Power and Controls" in IEEE Transactions on Industrial Informatics, vol. 14, no. 11, pp. 4940-4952, Nov. 2018

[7] G. Turner, J. P. Kelley, C. L. Storm, D. A. Wetz and W. -J. Lee, "Design and Active Control of a Microgrid Testbed" in IEEE Transactions on Smart Grid, vol. 6, no. 1, pp. 73-81, Jan. 2015

[8] C. Wang et al., "A Highly Integrated and Reconfigurable Microgrid Testbed with Hybrid Distributed Energy Sources" in IEEE Transactions on Smart Grid, vol. 7, no. 1, pp. 451-459, Jan. 2016.

[9] O. A. Mohammed, M. A. Nayeem and A. K. Kaviani, "A laboratory based microgrid and distributed generation infrastructure for studying connectivity issues to operational power systems" IEEE PES General Meeting, 2010, pp. 1-6

[10] J. Dannehl, C. Wessels, F.W. Fuchs, "Limitations of Voltage-Oriented PI Current Control of Grid-Connected PWM Rectifiers With *LCL* Filters", IEEE Transactions on Industrial Electronics 56, 2009, pp. 380–388.

[11] N. Menger, F. Sommer, T. Merz and M. Hiller, "Transient Power Control Algorithm for a Dual Active Bridge", 2021 23rd European Conference on Power Electronics and Applications (EPE'21 ECCE Europe), 2021, pp. 1-8.

[12] F. Sommer, N. Menger, T. Merz and M. Hiller, "Accurate Time Domain Zero Voltage Switching Analysis of a Dual Active Bridge with Triple Phase Shift", 2021 23rd European Conference on Power Electronics and Applications (EPE'21 ECCE Europe), 2021, pp. 1-9.

[13] R. Schwendemann, S. Decker, M. Hiller and M. Braun, "A Modular Converter- and Signal-Processing-Platform for Academic Research in the Field of Power Electronics", 2018 International Power Electronics Conference (IPEC-Niigata 2018 -ECCE Asia), 2018, pp. 3074-3080

[14] DIN EN 60297-3-101:2005-06, Construction methods for electronic devices - Dimensions of the 482,6-mm-(19-in-)construction - Part 3-101: Subracks and assemblies (IEC 60297-3-101:2004); German version EN 60297-3-101:2004

[15] B. Schmitz-Rode, L. Stefanski, R. Schwendemann, S. Decker, S. Mersche, P. Kiehnle, P. Himmelmann A. Liske and M. Hiller, "A modular signal processing platform for grid and motor control, HIL and PHIL applications", 2022 International Power Electronics Conference (IPEC), 2022, preprint

[16] R. W. De Doncker, D. M. Divan and M. H. Kheraluwala, "A three-phase soft-switched high power density DC/DC converter for high power applications", Conference Record of the 1988 IEEE Industry Applications Society Annual Meeting, 1988, pp. 796-805 vol.1

[17] R. Teodorescu, F. Blaabjerg, M. Liserre, P.C. Loh, "Proportional-resonant controllers and filters for grid-connected voltage-source converters" in IEE Proceedings - Electric Power Applications 153, 2006, pp. 750–762